

ACTUATED TENSILE TESTING OF CNT BASED ARCHITECTURES

Sebastian M. Geier¹, Thorsten Mahrholz¹, Peter Wierach¹, Michael Sinapius²

¹ German Aerospace Center (DLR), Institute of Composite Structures and Adaptive Systems
Lilienthalplatz 7, D-38108 Braunschweig, Germany
Sebastian.Geier@dlr.de

² Technical University of Braunschweig, Institute of Adaptronics and Function Integration
Langer Kamp 6, D-38106 Braunschweig, Germany

Keywords: Carbon nanotubes, CNT actuator, electrolytes, actuation mechanism, nanoscale actuation.

Summary: *Successful actuators have to meet a typically mechanical profile combining high flexibility and stiffness for bearing high structural loads. Current smart materials suffer from low or unstable mechanical properties. That is why these actuators are additionally fixed on structures and are used for the deflection process. In passive/uncharged status the actuators represent additional weight. In contrast to the mostly used piezo ceramic actuators (PZT) the new class of carbon nanotube actuators show promising electromechanical properties combined with low weight. Young's modulus of 640GPa and comparable high active strains of 1% seem to fulfill the requirements of a structural actuator. For characterisation paper-like architectures made of CNTs are tested in capacitor mode, two electrodes with an electrically insulating but ionically conductive electrolyte in between. An in-plane strain of the electrodes can be detected. However, the actuation-mechanism is still unknown. Different experiments point out different physical effects, ranging from electrostatic effects to quantum-mechanical effects. Actually it seems that the found results are a matter of the specimen, its composition and the type of experiment. The presented paper focuses on the results found during actuated tensile tests addressing dependencies between specimen composition and possible physical effects. Architectures made of single walled CNTs, also called CNT-papers and multi walled CNT-arrays, which feature single, continuous CNTs in one dimension, are compared. The tensile tests are conducted in dry, wet and wet/actuated condition to determine swelling effects. Furthermore tensile tests were conducted at different actuation potentials to identify an electrostatic effect. Different electrolytes are used too to be able to find a correlation between strain and ion radius. It can be found that the mechanical performance of the CNT paper strongly depends on the conditions. The Young's modulus is reduced by 40 %. In the case of actuation it is not as significant. However, reproducible results can be found by testing the CNT-paper sample in its elastic regime. As soon as charging begins an irreversible degradation of the stiffness can be detected. This points out a mechanical dependency to the charging maybe an effect of the ion radii. Also CNT-arrays seem to depend on the conditions. In terms of complete wetting CNT-arrays require ionic liquids due to their hydrophobic character while CNT-papers were tested in*

an aqueous electrolyte. According to the experimental conditions, the sample composition and the found electromechanical results a quantum-mechanical effect might probably be the reason for the array actuation.

1. INTRODUCTION

Iijima's publication in 1991[1] about rolled up graphitic sheets, also called carbon nanotubes, marks the beginning of the great scientific attention paid to this special carbon allotrope. Excellent electromechanical properties such as stiffness, strength, electrical and thermal conductivity seem to open up an almost endless number of applications [2, 3]. Beyond theoretical and applied scientific publications a commercially use turns out to be extremely challenging. One main reason might be the performance gap between nanoscale and macroscopic structures. However the rise of graphene since 2004 and unsolved quality problems at the CNT-synthesis [4] resulted in dwindling scientific interest but CNTs are still a prime candidate as nanotransistors for future super-fast computers [5].

Beside the mentioned excellent passive properties also the use of CNTs as electromechanical transducers generating free strain up to 0.2% was observed [6]. The CNT-papers are tested like a capacitor with a working electrode and counter electrode based on sheets of CNTs within an electrolyte. The analysed paper shows increasing deflections by increasing the charge independent of the polarity, positive or negative. Considering the mechanical properties this material seems to be promising for structural smart material. In contrast the latest active materials like piezo ceramics (PZT), shape memory alloys (SMA), shape memory polymers (PMA) or electroactive polymers (EAP) are either too brittle or too weak to transform forces or are simply too heavy for lightweight construction applications. In Figure 1 an overview of the most common active materials with their mechanical and active properties is given.

However, results like free strain or actuation force of CNT-based actuators have to be handled with care because they depend either on the analysed architecture made of CNTs or on the used analysis method. In this context the term *architectures* represents structures of macroscale dimensions formed by individual CNTs. The dimensions of CNTs are too small to form one dimension of the architecture by itself. Generally, the architecture bases on carbon tubes which are entangled with each other or linked by van der Waals forces. Thus results found by testing CNT-based architecture can only represent partially the active behaviour of the single tubes. Furthermore using out-of-plane set-ups to analyse CNT-papers in bending mode [6] give also rather qualitatively results because secondary effects like thermal- or diffusion-induced volume change can influence the findings extensively. For reducing these effects, the measurements are performed in the pre-stressed mode at the in-plane test set-up [7]. In this case the composition of the tested material has to be considered as symmetrical or homogeneous. However, various macroscale tests cannot give a satisfactory explanation for the effect as well as nanoscale analyses like atomic force microscopy of single tubes [8] or Raman-spectroscopy of CNT-papers [9]. Suppiger [10] deduced an electrostatic mechanism because of an inverse correlation between Young's modulus and free strain of CNT-papers. Furthermore Whitten [11] revealed strong dependencies between active performance and the test condition of the CNT-papers, whether

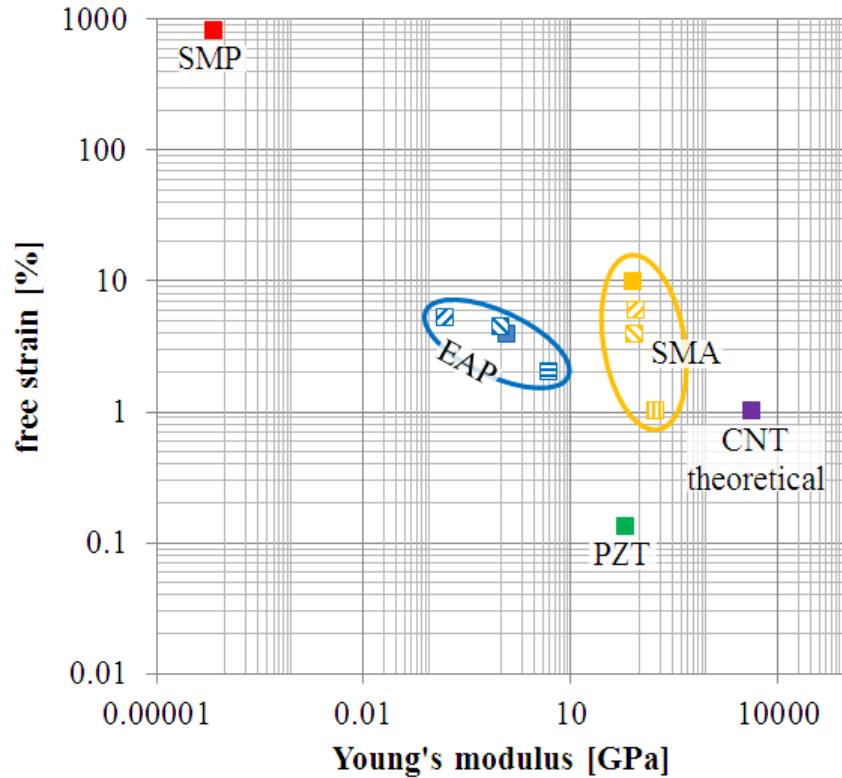


Figure 1: Overview of common smart materials with their electromechanical properties.

it is tested in dry or wet state. Especially using different types of electrolytes, aqueous solution vs. ionic liquid, indicates an influence of the ions. In addition Spinks [12] explained the deflections of CNT-papers by their composition similar to honeycombs, which swells by ion-diffusion. Thus CNT-papers seem to be rather influenced at their tube linking instead of transferring a reaction of the CNT-structure. In contrast CNT-arrays might be an alternative which already reach microscale dimensions in terms of tube length what makes them handable for testing. Yun [13] actuated towers of CNTs, a comparable term for arrays, to measure their active performance. Unfortunately the weak mechanical linking between the tubes and the silicone substrate as well as the curly shape of the individual tubes reduces the significance of the results in order to clarify the mechanism of the observed actuation. Further research [14] compares different types of arrays according to their morphology and quality of orientation in order to find a correlation to their active behaviour and significance. It was found that the quality of orientation is an important fact for accurate describing of the actuation and avoiding secondary effects. In the presented paper two types of samples are comparably tested in order to clarify their electromechanical dependencies and actuation-mechanism. On the one hand the already mentioned CNT-papers are investigated in detail to define the decisive parameters for actuation. The CNT-papers are made of single walled CNTs (SWCNTs). On the other hand CNT-arrays are tested the same way. The arrays are consisting of multi-walled CNTs (MWCNTs). It is

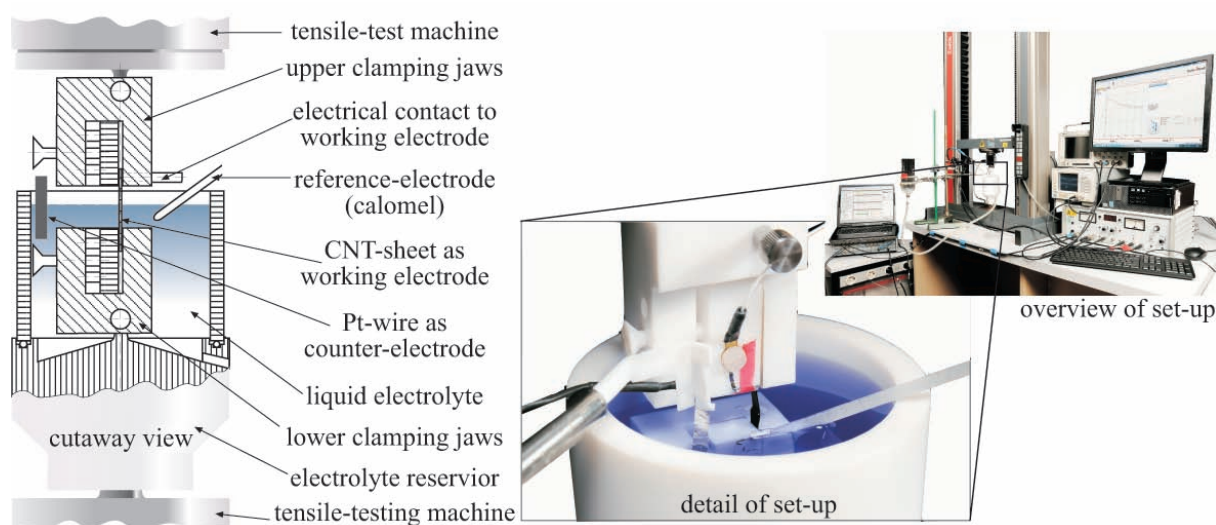


Figure 2: Schematic sectional sketch, overview and detail view on the real test set-up of actuated tensile test.

expected that a comparison of the electromechanical results of both sample types (CNT-paper vs. CNT-arrays) will reveal their individual condition related behaviour and differences in terms of composition and charged-induced active behaviour.

2. EXPERIMENTAL

In the following chapter the test set-up, the testing procedure, the specimen preparation and the used calculations are presented.

2.1 SET-UP OF THE ACTUATED TENSILE TEST AND TEST PROCEDURE

Core part of the actuated tensile test is a standard tensile test facility (Z005, Zwick GmbH & Co. KG) which is supplemented by two clamping jaws made of polytetrafluorethylene (PTFE) and a housing for wetting the samples with electrolyte during performing the experiment. PTFE is electrochemical inert during charging the samples what avoids contamination of the electrolyte by chemical reaction with e. g. rust of ignoble parts. However, it is clear that PTFE is a comparable soft material with which the CNTs cannot be tested to their extreme. The aim of these experiments is a qualitative comparison of samples made of two different types. A schematic picture and a detailed view of the test set-up is shown in Fig. 2. The tests are conducted with a speed of 0.03 mm/min to avoid preimparments. For a sufficient resolution a 10 N load cell (KAP-Z, Zwick GmbH & Co. KG) is used. Due to the precision of the controlling methods and to avoid a premature failure of specimens the tests are conducted path controlled. Therefore force based results are recorded. The force and range of movement are recorded by the software TestExpert II V3.31, also provided by Zwick.

The CNT-samples are arranged similar to an in-plane strain test set-up which is described elsewhere [7]. Within the three electrode cell the CNT-sheet represents the working electrode. For reasons of reproducibility a Pt-wire works as counter electrode. A calomel electrode (KE 10, Sensortechnik Meinsberg GmbH) corresponds to the reference electrode. The working and the counter electrode are arranged like a capacitor with the reference electrode in between but positioned closer to the working electrode. All electrodes are immersed in a specimen-specific electrolyte which is described later. The cell is controlled by a potentiostat (1030 PC.T., IPS Elektroniklabor GmbH & Co. KG) and can be charged via a function generator (FG 300, Yokogawa Deutschland GmbH). The results are recorded via a data acquisition system (SCM05, LMS International). Both clamping jaws are equipped with electrodes for detecting the electrical resistivity of the sample indicating a damage of the specimen during mounting or an inaccurate clamping.

While former tests are conducted under varying conditions to prove condition-induced electromechanical properties the presented results focus on reproducible tensile tests of CNT-papers within their elastic range. Former tests showed wide standard deviation of the Young's modulus in their charged statuses which were difficult to discuss because possible effects are not obviously any more. In the presented campaign the specimen are immersed in their individual electrolyte for at least 30 minutes to be saturated with ions and to avoid material swelling during the test what can wrongly also interpreted as active behaviour. The clamping length is individually manipulated that way that all tests start with unloaded specimens. The specimen are charged constantly during the whole test and loaded until an uncritical force. This procedure is repeated for at least six times using the same voltage step and then continued using higher steps within the voltage-range of their redox-window for negative and positive potentials around the zero potential of 0.1 V. The Young's moduli of the different steps are compared afterwards.

2.2 SAMPLE PREPARATION AND TESTING DETAILS

A CNT-paper can be produced as result of a multiphase process starting with an aqueous solution containing 99 g deionized water, one gram surfactant (sodium dodecyl sulfate, SDS, with a purity of 99 % supplied by Sigma-Aldrich Co. LCC.) and 0.1 g SWCNT-powder (Elicarb 0925, Thomas Swan Ltd.). The CNTs are homogenized by an ultrasonic bath (Sonorex Digital 10P with maximum power, Bandelin Electronic GmbH & Co. KG) for 180 minutes. Hereafter the prepared CNT-suspension is filtrated under pressure of 6 bar and deposited on a polycarbonate membrane containing pores of 400 nm (Track-Etche polycarbonate membrane 23006-47, supplied by Satorius AG). The sheet is rinsed with 600 ml deionized water in order to remove the surfactant. Afterwards the paper can be peeled off the membrane and is pressed within a PTFE-based mold by 1.87 Pa in an oven at 80°C (UFP 500 M1 T 300C, Memmert GmbH & Co. KG) for at least four hours. The upper and lower surfaces of the sheets are analysed selectively by scanning electron microscopy (LEO 1550, Zeiss Jena AG, working distance of 7 mm, operating voltage of 5 kV). The CNT-sheets are constantly charged during the whole test using voltage steps of $\Delta \pm 0.5$ V and $\Delta \pm 0.9$ V according to their redox-window of ± 1 V. The papers are preloaded until 0.015N while the Young's moduli are calculated between 0.04

Table 1: Overview of crystalline and hydrated ion radii used for aqueous electrolytes.

ion	crystalline radius [pm]	hydrated radius [pm]
Cl^-	181	332
Na^+	95	358
K^+	133	331

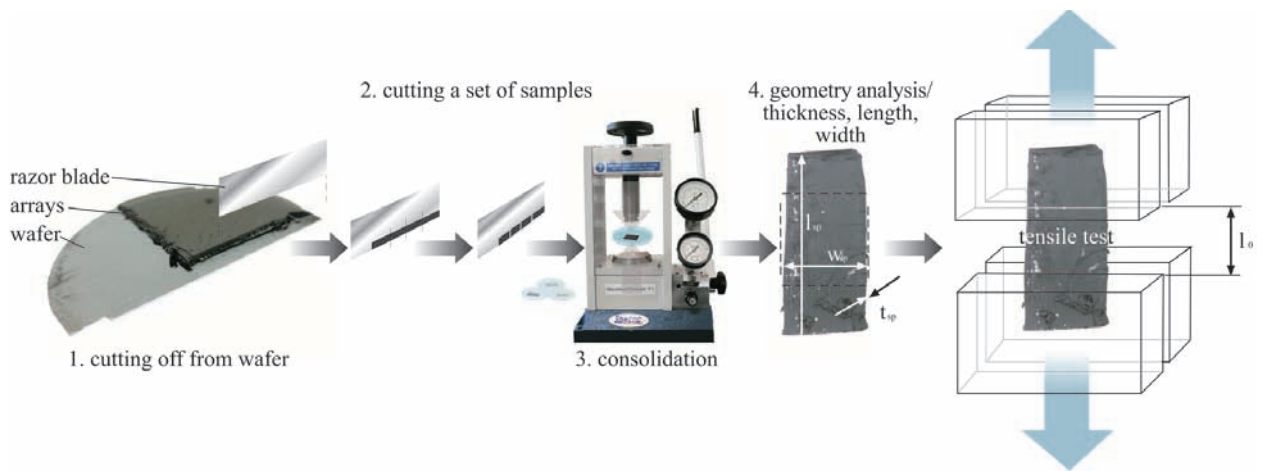


Figure 3: Schematic manufacturing process of CNT-array samples.

N and 0.14 N. In order to avoid high standard deviations due to a varying quality of different CNT-papers the tested samples are cut off only one CNT-paper. The average CNT-paper sample geometry is 1.5 mm in width the free length between the clamping jaws are 5 mm which is manipulated individually to provide a preload-free condition for each CNT-paper as initial state. According to different ion-types [15] and their influence on the modulus a one molar sodium chloride solution and a one molar potassium chloride solution are used and their results are compared. Nightingale measured the crystalline and hydrated ion radii of sodium, potassium and chloride (see Table 1). By using the same negative ion, the influence of the positive ion radius should be obviously.

The MWCNT-arrays are supplied by the Technical University of Hamburg-Harburg (TUHH, Germany) on a silicon wafer. These arrays are grown within 5.5 hours using a standard thermal chemical vapor deposition process (CVD). The quality of tube orientation and variation of tube diameter is analysed by SEM. According to the dimensions of CNT-arrays a special preparation process has to be applied (see Fig. 3).

In a first step a complete cross section of the array is cut off by a sharp razor blade. The as-produced specimen thickness is about 1 mm. In a following step the cross section is divided into a set of specimens with almost the same width. To remove those samples from the razor blade a tweezer has to be used carefully. In terms of consolidation the sample is positioned between two microscope slides and pressed so that a sample can be compacted by 80-97 %. Further compacting can be achieved via a manual hydraulic press (Atlas manual 25 tons hydraulic press GS25011, Specac Limited, UK) by applying 10 tons what means a averaged pressure of 10895MPa. The results are also analysed via SEM.

A digital microscope (VHX-1000, Keyence Corporation) is used to measure the exact two dimensional sample geometry such as length and width. The thickness is analysed using a micrometer screw (IP 54, Mitutoyo Europe GmbH). To avoid structural damage the samples are positioned between two glass-slides during the measurement. Contact angle measurements reveal the array's superhydrophobic character (Contact Angle System OCA 20, Data-Physics Instruments GmbH) what is the reason for using an ionic liquid as nonpolar electrolyte. Further measurements showed high capacitive potentials for 1-ethyle-3-methylimidazolium bis(trifluormethyl-sulfonyl)imide (EMImTfSA, IoLiTec GmbH) and a comparably large redox window with a range of ± 2 V. Here voltage steps of $\Delta \pm 1$ V $\Delta \pm 1.5$ V are used. The array samples are preloaded during activation with 0.45 N. The specimen geometry ranges between 4-5 μm in thickness and 4-4.6 mm in width with a free length between the clamping jaws of 1 mm.

2.3 MATHEMATICAL FORMULA

The Young's modulus E of the material is calculated by the stress σ_n using the measured force F_n and the specimen cross section geometry w_{sp} and t_{sp} (compare equation 1[16]). As second parameter the relative strain ε_n is calculated using the detected displacement Δl_{sp} , see equation 2[16]. Finally E is calculated between all measured points by equation 3. The experiments are only conducted in the linear-elastic region of the CNT-sheets. The presented Young's modulus is an averaged result of the whole graph.

$$\sigma_n = \frac{F_n}{A_{sp}} = \frac{F_n}{w_{sp} \cdot t_{sp}} \text{ [MPa]} \quad (1)$$

$$\varepsilon_n = \frac{\Delta l_{sp}}{l_0} \text{ [%]} \quad (2)$$

$$E = \frac{\Delta \sigma}{\Delta \varepsilon} \text{ [MPa]} \quad (3)$$

A_{sp}	$[m^2]$	specimen's cross-section area
E	$[Pa]$	Young's modulus
σ_n	$[Pa]$	mechanical stress
ε_n	$[\%]$	relative strain
F_n	$[N]$	force during test
l_0	$[m]$	free distance between clamp jaws
w_{sp}	$[m]$	width of sample
t_{sp}	$[m]$	thickness of sample

3. RESULTS AND DISCUSSION

Firstly the quality assessment of CNT-papers and CNT-arrays are presented followed by the results of the actuated tensile tests of CNT-papers and finally CNT-arrays.

QUALITY ASSESSMENT OF THE SAMPLES

From SEM images of the CNT-paper surface no detailed information about the paper composition is received because of highly compacted material. Thus, only SEM-images of the CNT-paper fracture line, as it is presented in Fig. 4 a), can reveal a layer-like build-up, similar to findings documented by Spinks [12]. The layers may result from mass induced sedimentation of the homogenized CNT powder during the filtration process what indicates that the paper composition cannot be considered as symmetrical. While single CNTs are almost not visible at the top and bottom side of the paper the top view on the fracture line in Fig. 4 b) illustrates bundles of SWCNT which are aligned due to tensile forces.

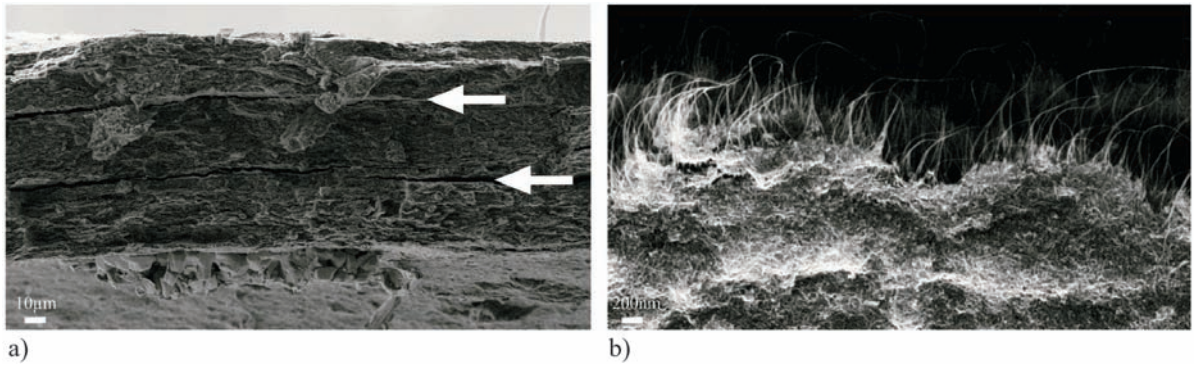


Figure 4:

- a) Sectional SEM image of a CNT-paper fracture line with a build-up containing three main layers (se).
- b) Top view on aligned SWCNTs at the fracture line as consequence of the tensile testing (in-lens).

The average specific conductivity of 169 S/cm on the top side (compacted by water) indicates a good entanglement of the SWCNTs. The rear side features a slightly lower averaged specific conductivity of 167 S/cm. The conductivity varies in the range of 203-145 S/cm what is an effect of electronic conduction as result of a compact composition. The thickness varies between 193-115 μm . A correlation between thickness and conductivity cannot be found because both distributions are completely different in terms of a convex thickness distribution with a maximum thickness of 0.19 mm in its middle vs. a linear conductivity gradient from one side to the other. SEM-analyses of the tested samples in comparison of the dry, untested samples indicate an irreversible swelling of the paper as it is shown in Fig. 5.

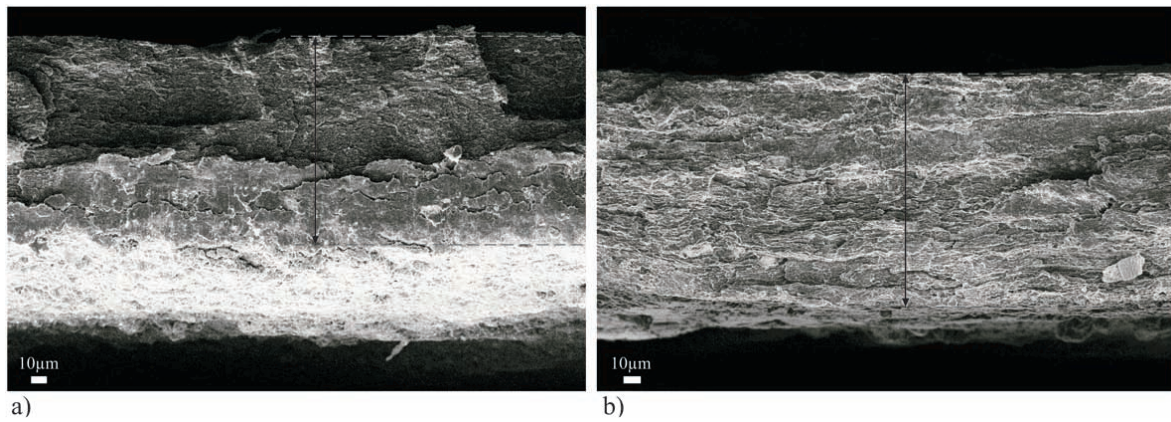


Figure 5:

- a) SEM image of the dry paper (inlens).
- b) SEM image of the CNT-paper after actuated testing (inlens).

Analyses of the thicknesses before and after testing reveal a swelling of 12.5 % of the paper architecture as result of charging and ion diffusion. SEM analyses (compare Fig. 6 a) of CNT-arrays showed an average length l_{cnt} of 2200 μm with slightly varying average diameters of 20 nm as it can be seen in Fig. 6. The CNT-curvature varies along the array length and width (compare Fig. 6 c). For the following tensile tests the waviness provides the opportunity to align the sample by preloading within the test before destroying the sample. Checking the stress-graph carefully will help to find the state in which almost all CNTs are aligned.

The following SEM-images 7 a), b) show the result of CNT-arrays compacted by hydraulic pressing. Obviously spaces of the as produced array in a) can be reduced comparing image b) while the orientation can mainly be preserved. However, at tested specimen also areas of failure of the CNT structure can be found (Fig. 7 c). The multi-walled CNTs are mostly broken perpendicular to their axis. This indicates an extreme, external impact which probably appears in or near to the clamping jaws where the CNTs are fixed.

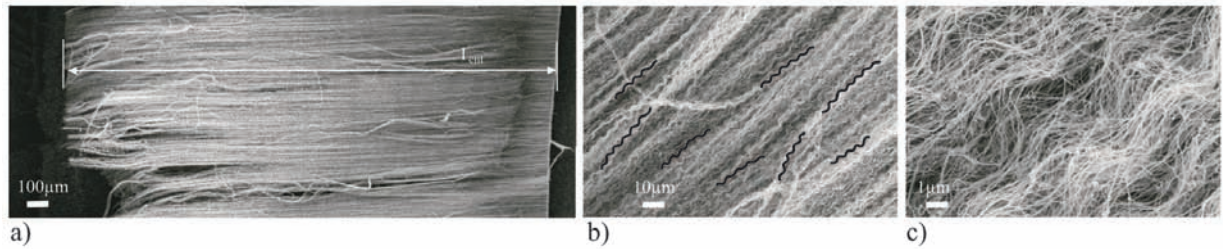


Figure 6:

- a) SEM image of the overall length of an array (inlens).
- b) Image with higher resolution for a better view on the waviness (inlens).
- c) Detailed view on curly CNTs (inlens).

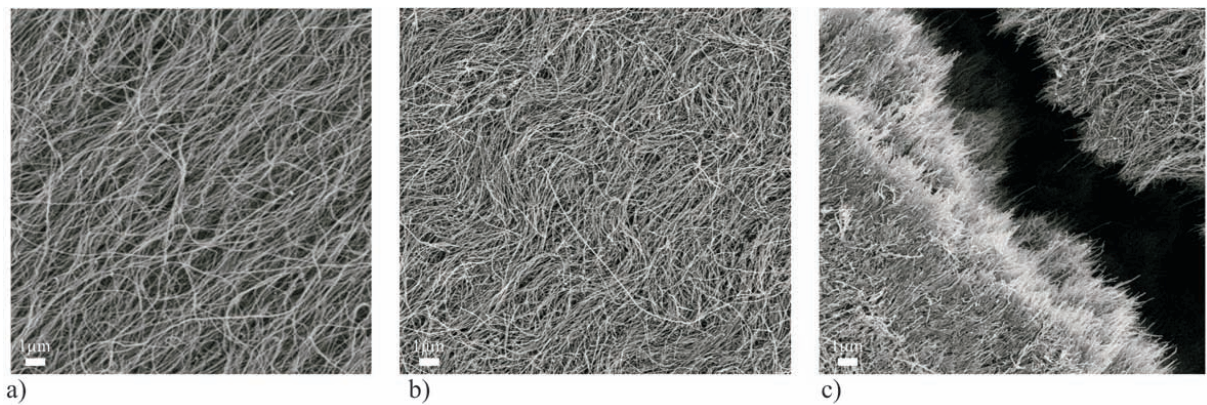


Figure 7:

- a) Detailed SEM image of as produced CNT-arrays bundles (inlens).
- b) Detailed image of arrays compacted by the hydraulic press (inlens).
- c) View on a fracture line of a failed array sample (inlens).

3.1 RESULTS OF ACTUATED CNT-PAPER TEST

As mentioned further test results already document the breakdown according to an increasing wetting of the papers. The specific values are given in Table 2. As it can be seen by the standard deviations especially at the actuated states a significant conclusion is limited. Actually a CNT-paper actuator should work in reversible manner. Furthermore the set-up is not designed for testing CNT-paper at their mechanical extremes. Therefore the procedure was adapted in terms of better reproducibility and lower standard deviations.

Table 2: Overview of test results recorded during the tensile tests of CNT-papers

test condition	number of specimens	averaged Young's modulus [MPa]	standard deviation [%]	best Young's modulus [MPa]
dry	13	356	33	621
wet	10	198	33	299
wet at +0.5 V	12	152	60	276
wet at +0.9 V	4	147	69	274
wet at -0.5 V	3	228	16	265
wet at -0.9 V	3	270	8	292

In the following experiments CNT-papers are tested within their elastic regime. That way a reversible experiment can be expected. In Fig. 8 a) and b) the averaged mechanical results of CNT papers, one immersed in an aqueous one molar NaCl solution and another in a one molar KCl solution, are presented. The specific value can be found in Table 3. The presented graphs are zoomed because the differences between the charged states are very small.

It can be seen that the Young's modulus falls by charging regardless of the electrolyte. Another aspect is the relations of the decreasing modulus. Both times the negative charged anion has a bigger impact on the modulus than the positive cations at the same Δ potential. As it can be expected that the modulus reduction correlates with the increasing Δ potential. Using sodium chloride the modulus stays almost the same at -0.4 V but falls by 2.3 %. At positive potentials +0.6 V generates a loss of 1.4 %, +1 V a loss of 46 %. It has to be mentioned that this latter result was only repeated once. It seems that the modulus can be more affected by the Cl^- -ion than by the sodium or potassium ions. At -0.4 V a loss of 2.3 % can be detected while higher negative potentials remain on this level. Positive potentials almost remain on the same level. Only higher potentials can cause a further reduction of 2 %.

It is demonstrated that a CNT-paper can be tested with reproducible results in its elastic regime but in combination with an electrical charging the structure is irreversibly manipulated

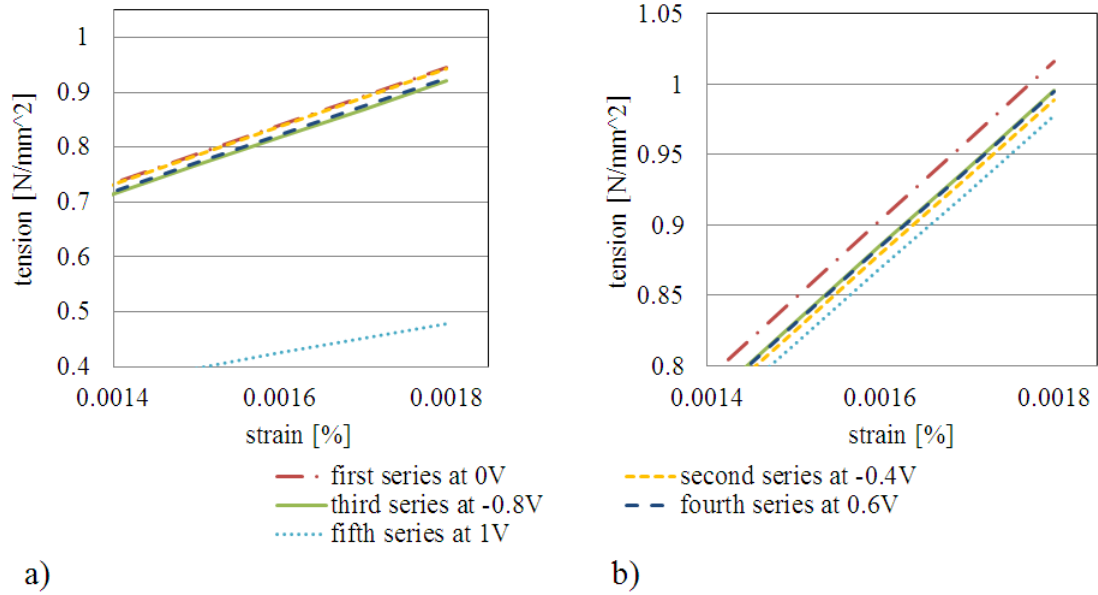


Figure 8:

- a) Detail of averaged stress-strain graph of a CNT-paper in an one molar NaCl solution.
 b) Detail of averaged stress-strain graph of a CNT-paper in an one molar KCl solution.

towards lower mechanical stiffness. Although intermediate steps of the already mentioned tests were performed in which the sample was uncharged again the initially values could never been reached again (see Fig. 9 a). Moreover the results remained on the level of the previous, charged test with slightly mechanical recovery. However the sample was not destroyed by these tests. A tensile test can still be carried out revealing a remarkable mechanical residual strength as it is shown in Fig 9 b). In total the effect of the Cl⁻-ion seems to be more dominant comparing to its positive counterparts. Considering the radii of Table 1 the crystalline radius seems to be the decisive parameter. With these considerations and according to the radii of the positive ions Na⁺ and K⁺ the latter one should generate bigger effects. This correlation cannot be found here. However more tests have to be carried out to prove if the radius may be the explanation for the actuation of CNT-papers.

3.2 RESULTS OF CNT-ARRAYS TESTED BY ACTUATED TENSILE TESTING

In contrast to the randomly oriented architectures such as CNT-papers, arrays enable to focus on the CNT-structure because the sample contains single and continuous CNTs in that dimension in which it is analysed. The curly shape can be considered as a micro-spring providing a mechanical backup to avoid the sample's failure. Once the spring is stretched to the maximum an almost perfect alignment can be expected. The challenge is to identify this point and to carry out all active measurements. Fig. 10 presents the modulus shift induced by the

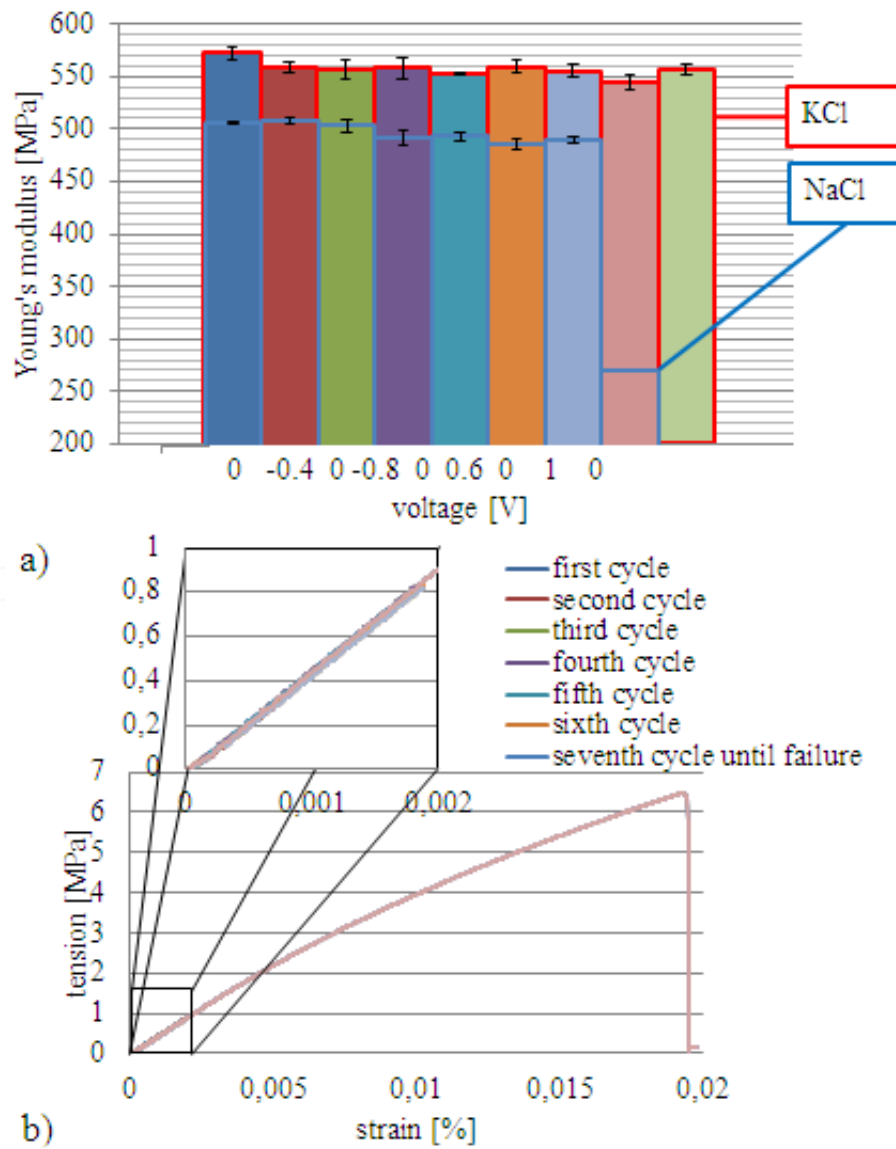


Figure 9:

a) Comparison of the measured CNT-paper moduli.

b) Tensile test until failure after 29 charged tensile tests conducted in the elastic regime with a detailed view on the elastic regime. Only four elastic tests are presented

Table 3: Overview of results during charging and elastic tensile testing

volts	number of cycles	NaCl-solution		KCl-solution	
		averaged Young's modulus [MPa]	standard deviation [%]	averaged Young's modulus [MPa]	standard deviation [%]
0 V	6	529	0.3	571	1.1
-0.4 V	6	531	0.7	559	0.9
-0.8 V	6	515	1.4	558	1.6
+0.6 V	6	508	1.1	559	1.2
+1 V	6	276	-	554	1.4

conditioning. Beginning with a Young's modulus of 41 MPa the wetting reduces the modulus by 50 % to a value of 22 MPa. Further treatment (cycling with 0 V) causes again a reduction of the modulus down to 14 MPa. The actuation generates no further decreasing of the modulus. However, previous tests came to different findings - almost constant moduli regardless of the condition - so that more test have to be carried out to prove the mechanical behaviour of arrays under wet and actuated conditions.

The ionic liquid EMImTFSa provides a redox window of -2.5 V to 2 V for avoiding irreversible chemical reactions but as result of the cyclic voltammetry the used voltage range is reduced to ± 1.5 V. Current peaks document oxidation- and reduction-reactions destroying mostly the electrolyte what is not desirable for a long lifetime of an nano actuator. According to the higher resolution of the load cell the generated force was recorded. In Fig. 11 all results of the array-actuator activated by -1.5 V and 1.5 V are presented. Both graphs of the current as well as the charge confirm the actuator set-up to be capacitive with only a tiny share of current leakage. It can be seen, that both potentials generate forces but with different shapes. While the force peak generated by a negative potential seem to be almost constant during the charging with sharp edges what indicates a very fast process the force response of the positive potential shows gradients during charging and discharging. This result might represent an even more slowly, diffusion dominated process. Due to the fact that the molecular structure of ions is more complex in contrast to the aqueous electrolytes the ion radius can hardly be considered as explanation until now.

If the arrays can be considered as aligned tubes generating an elongation during charging the ion radius should have no impact. However, the values of the generated forces according to the different potentials -1.5 V and at 1.5 V are the same: 0.0015 N what supports the expectation. Maybe both ions are of different ion flexibility enabling different accessibility onto the carbon surface, the results - an elongation instead of a contraction - as well as the sample composition

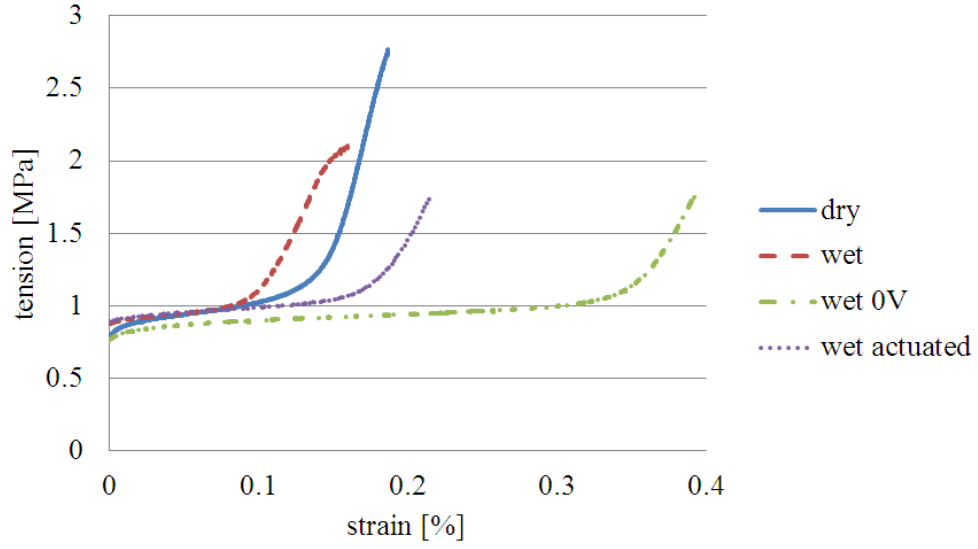


Figure 10: Stress-strain curves of the actuated array under tensile testing and at different conditions.

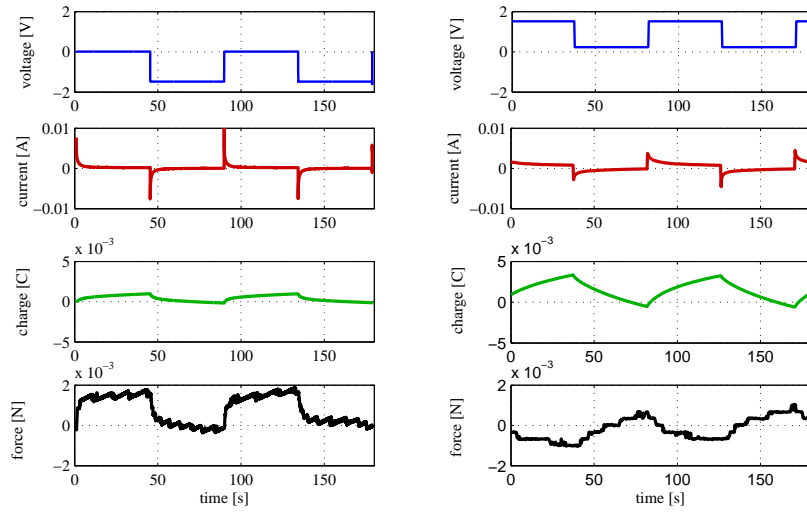


Figure 11: Voltage step, current, charge and force graphs at -1.5V and +1.5V.

- aligned, pre-loaded long CNTs - point out quantum mechanical reasons for the actuation of CNT-arrays.

4. CONCLUSION

This paper presents a actuated tensile test of two different types of carbon-based specimen. Although both kinds of specimens, CNT-papers with randomly oriented SWCNTs and arrays containing highly aligned MWCNTs, reveal different morphology they show a similar trend of the mechanical behaviour according to different conditions. While the measurements of the CNT-paper are focused on their charged induced stiffness degradation by testing those within their elastic regime the CNT-arrays are analysed in terms of active behaviour. With very low standard deviations it can be shown that CNT-papers are sensitive to the charging. Regardless the polarisation a degradation of up to 50 % can be detected. Moreover the experiments point out a stronger manipulation by the negative charged anion Cl^- because of bigger degradation. Concerning the ion radius as the decisive parameter only the crystalline value fits the findings. A comparison of the positive cations in terms of ion-radius sensitivity is not as clear until now. In contrast the CNT-arrays also show a condition induced mechanical degradation by 50 % what is in contrast to results of further measurements. Here more measurements have to be carried out for getting a reliable statement. During the actuated tensile tests an active performance at negative and positive potentials can be found. Nonetheless the test set-up, the specimen composition and the results - force degradation during charging - indicate strongly a quantum mechanical effect as reason for actuation. Both tests point out further potentials in defining the different mechanisms but also suffer from low statistical relevance in terms of number of samples. A challenge that will be taken up in the future work of this project.

5. ACKNOWLEDGEMENTS

This work is part of the basic research on future smart materials at the DLR - Institute of Composite Structure and Adaptive Systems. It was supported by the German Research Council (DFG) within the framework of the DFG PAK 355 - 'Basics for CNT-based Actuators' and the German Federal Ministry of Education and Research (BMBF) project 'Aktu_Komp'. Tribute has also to be paid to the colleagues at the Institute of Composite Polymers at the Technical University Hamburg-Harburg for their contribution in the fields of CNT-materials and the Institute of Mechanical Process Engineering, department of Interface Chemistry at the Technical University of Clausthal-Zellerfeld for their expertise-support in terms of ionic liquids.

References

- [1] S. Iijima, Helical microtubules of graphitic Carbon. *Nature*, **354**, 56-58, 1991.
- [2] L. Forro, et al., Electronic and Mechanical Properties of Carbon Nanotubes. *Science and Application of Nanotubes*, **Part III**, 297-320, 2002.

- [3] M.-F. Yu, O. Lourie, M. J. Dyer, K. Moloni, T. F. Kelly, R. F. Ruoff, Strength and Breaking Mechanism of Multiwalled Carbon Nanotubes Under Tensile Load. *Science*, **287**, 637-640, 2000.
- [4] N. Grobert, Nanotubes - grow or go? *Mater. Today*, **9(10)**, 64, 2006.
- [5] F. Kreupl, Electronics: Carbon nanotubes finally deliver. *Nature*, **484**, 321-322, 2012.
- [6] R. H. Baughman et al., Carbon nanotube actuators. *Science*, **284**, 1340-1344, 1999.
- [7] J. Riemenschneider, H. Temmen and H. P. Monner, CNT based actuators: Experimental and theoretical investigation of the in-plane strain generation. *J. Nanosci. Nanotech.*, **7(10)**, 3359-3364, 2007.
- [8] A. Minett, J. Fraysse, G. Gang, G.-T. Kim, S. Roth, Nanotube actuators for nanomechanics. *Curr. Appl. Phys.*, **2**, 61-64, 2002.
- [9] S. Gupta, M. Hughes, A. H. Windle, J. Robertson, In situ Raman spectro-electrochemistry study of single-wall carbon nanotubes mat. *Diam. Relat. Mater.*, **13**, 1314-1321, 2004.
- [10] D. Suppiger, S. Busato, P. Ermanni, M. Motta, A. Windle, Electromechanical actuation of macroscopic carbon nanotube structures: mats and aligned ribbons. *Phys. Chem. Chem. Phys.*, **11**, 5180-5185, 2009.
- [11] P. G. Whitten, G. M. Spinks, G. G. Wallace, Mechanical properties of carbon nanotube paper in ionic liquid and aqueous electrolytes. *Carbon*, **43**, 1891-1896, 2005.
- [12] G. Spinks, G. G. Wallace, L. S. Fifield, L. R. Dalton, A. Mazzoldi, D. De Rossi, I. I. Khayrullin, R. H. Baughman, Pneumatic Carbon Nanotube Actuators. *Adv. Mater.*, **14(23)**, 1728-1732, 2002.
- [13] Y.H. Yun, V. Shanov, Y. Tu, M. J. Schulz, S. Yarmolenko, S. Neralla, J. Sankar, S. Subramaniam, A Multi-Wall Carbon Nanotube Tower Electrochemical Actuator. *Nano Lett.*, **6(4)**, 689-693, 2006.
- [14] , S. Geier, T. Mahrholz, P. Wierach, M. Sinapius, Carbon nanotubes array actuators. *Smart. Mater. Struct.*, **22(9)**, 094003, 2013.
- [15] E. R. Nightingale, Phenomenological Theory of Ion Solvation. Effective Radii of Hydrated Ions. *J. Phys. Chem.*, **63(9)**, 1381-1387, 1959.
- [16] J. Wittenburg, E. Pestel, *Festigkeitslehre, Ein Lehr- und Arbeitsbuch*. Springer, Berlin, Heidelberg, New York, **ed. 3** 2001.